Journal of Fluids and Structures (2000) **14,** 575–592
doi:10.1006/jfls.1999.0285, available online at http://www.idealibrary.com on IDEAL®

SECOND-ORDER WAVES IN A THREE-DIMENSIONAL WAVE BASIN WITH PERFECTLY REFLECTING SIDEWALLS

W. Li and A.N. Williams

Department of Civil and Environmental Engineering, University of Houston Houston, TX 77204-4791, U.S.A.

(Received 22 September 1998, and in final form 25 October 1999)

A complete second-order solution is presented for the three-dimensional wave field produced by the snake-like motion of an array of wave generators located at one end of a semi-infinite rectangular tank. The solutions to the boundary-value problems at first and second order are obtained by the method of eigenfunction expansions and are correct to second order in wave-maker stroke (wave amplitude). This frequency-domain solution may be considered as an extension of the earlier (1991) two-dimensional (narrow flume) solution of Hudspeth & Sulisz. Numerical results are presented that illustrate the influence of the various wave maker and basin parameters on the generated wave field.

1. INTRODUCTION

In certain applications, wave directionality plays an important role in the hydrodynamic loading experienced by coastal and ocean structures. To address this issue, many experimental facilities consist of a relatively wide wave basin in which directional seas can be produced by the prescribed motion of an array of wave generators located along one or more of the basin walls. The generated wave field is produced based on the snake principle, namely that the spatially sinusoidal motion of an infinitely long wave maker will produce regular waves which propagate obliquely to the generator plane [see, for example, Dean & Dalrymple (1984)]. However, the finite width of the basin results in the waves produced by this technique being influenced by sidewall reflections and any interpretation of the results from this type of laboratory facility must take this reflection into account. Funke & Miles (1987) discuss an extension of the snake principle to account for the effects of finite tank width. Dalrymple (1989) applied the mild slope equation to predict the wave field generated by snake-like wave maker motions in a finite basin with fully reflecting sidewalls. He also determined the modified wave generator signal necessary to obtain desired wave conditions at a specified distance from the wave makers, including sidewall reflections. The directional wave field produced by an array of wave generators moving according to the snake principle has been studied by Isaacson(1995) using a boundary element approach, and by Williams & Crull (1996) using a tank Green function which explicitly satisfies the no-flow conditions at the sidewalls. These latter two studies have also examined the influence on the wave field of placing a vertical cylinder in the test area of the basin.

However, all of the above solutions assume small-amplitude wave-maker motions and so are of limited usefulness when dealing with more extreme wave conditions. In order to predict the nonlinear wave field produced by finite-amplitude wave-maker motions, several investigators have approached the problem using the Stokes expansion procedure, keeping

0889–9746/00/050575 + 18 $35.00/0

terms up to second order in wave-maker stroke. Up to the present time, second-order solutions for wave motions have been restricted to two dimensions, which corresponds to a narrow tank, or flume, and a planar wave maker. Madsen (1971) presented an approximate solution for the second-order wave field produced by a planar wave maker in which the effect of the first-order evanescent wave field was neglected, therefore his solution is valid for long waves. Daugaard (1972) and Flick & Guza (1980) have presented other approximate second-order solutions for piston and flap-type wave makers, respectively. Ottesen-Hansen *et al.* (1980) and Sand (1982) discussed the elimination of spurious second-order wave components by imposing compensating second-order wave-maker motions. Sand & Mansard (1986) extended the approach and presented a technique necessary to produce the correct higher harmonics in an irregular sea state. Hudspeth & Sulisz (1991) and Sulisz & Hudspeth (1993a, b) presented a complete second-order frequency-domain solution for the wave fields produced by the monochromatic oscillations of both flap- and piston-type wave makers by an eigenfunction expansion approach. Their solution has been extended to deal with bichromatic wave-maker motions by Moubayed & Williams (1994) and, more recently, by Schaffer (1996). Zhang & Williams (1996, 1999) have presented second-order time-domain solutions for monochromatic and bichromatic wave-maker motions, with particular focus on developing appropriate radiation conditions for the second-order wave components.

Any extension of the existing two-dimensional analyses to provide a wave generator signal to eliminate spurious second-order wave components in a three-dimensional wave basin requires as a first step a complete second-order wave-maker solution for this geometry. Such a solution will be presented herein, where a complete second-order theory is developed for the three-dimensional wave field produced by the snake-like motion of an array of wave generators located at one end of a semi-infinite rectangular tank. The solutions to the boundary-value problems at first and second order are obtained by the method of eigenfunction expansions and are correct to second order in wave-maker stroke (wave amplitude). The solution is validated by comparison with two limiting cases, namely the first-order three-dimensional solution of Williams & Crull (1996) and the second-order two-dimensional solution of Hudspeth & Sulisz (1991). Then, numerical results are presented that illustrate the influence of the various wave maker and basin parameters on the generated wave field, in particular the influence of wave angle and basin width is investigated.

2. THEORETICAL DEVELOPMENT

A segmented wave generator occupies one wall of a semi-infinite rectangular basin of width b and constant water depth h. Cartesian coordinates (x, y, z) are employed with the x- and y-axis in the horizontal plane. The z-axis is directed vertically upwards from an origin on one tank wall at the still water level, i.e. the tank walls are located at $y = 0$ and $y = \mathrm{b}$ (Figure 1). The wave generators are assumed to undergo a prescribed small-amplitude oscillation of frequency ω, so that the associated fluid motion may be described by Stokes wave theory. Under the assumption of an inviscid, incompressible fluid undergoing irrotational motion, the wave motion may be described in terms of a velocity potential $\Phi(x, y, z, t)$ such that the fluid velocity vector $q = \nabla\Phi$. The fluid velocity potential, free-surface elevation, $\eta(x, y, t)$, and Bernoulli constant, $B(t)$, are assumed expressible in Stokes series, that is

$$\Phi(x, y, z, t) = \varepsilon\Phi^{(1)}(x, y, z, t) + \varepsilon^2\Phi^{(2)} + \ \dots\,, \tag{1}$$

$$\eta(x, y, t) = \varepsilon\eta^{(1)}(x, y, t) + \varepsilon^2\eta^{(2)} + \ \dots\,, \tag{2}$$

$$B(t) = \varepsilon B^{(1)}(t) + \varepsilon^2 B^{(2)} + \ \dots\ . \tag{3}$$

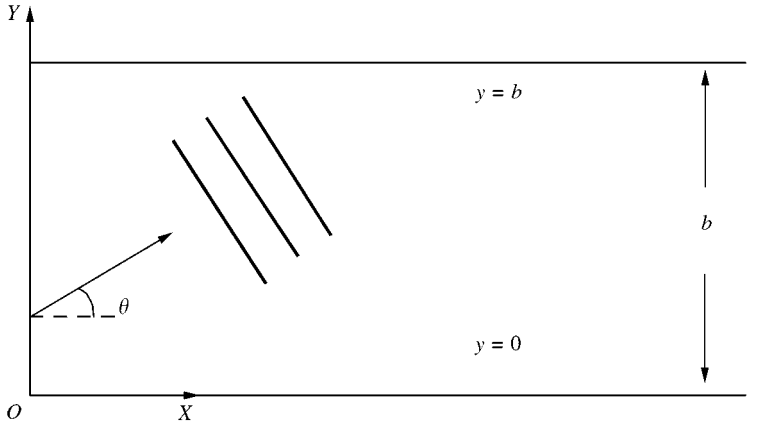

Figure 1. Definition sketch.

The horizontal wave-maker displacement about the mean position, $x = 0$, is given by

$$X(y, z, t) = \varepsilon f(z)\, e^{i(\lambda_0 y - \omega t)} + \text{CC}, \tag{4}$$

where CC implies the conjugate part of the preceding expression, $f(z)$ is the (real) wave-maker shape function, and λ_0 is the y-component of the wavenumber of the desired waves, defined by $\lambda_0 = \gamma_0 \sin\theta$ where θ is the angle the waves make with the x-axis, and the wavenumber γ_0 satisfies the linear dispersion relation $\omega^2 = g\gamma_0 \tanh \gamma_0 h$.

The first-order problem, at $\mathcal{O}(\varepsilon)$, is given by

$$\nabla^2 \Phi^{(1)} = 0 \quad \text{for } x \geq 0, \ -h \leq z \leq 0, \text{ and } 0 \leq y \leq b, \tag{5}$$

$$\frac{\partial \Phi^{(1)}}{\partial z} = 0 \quad \text{for } x \geq 0, \ z = -h, \text{ and } 0 \leq y \leq b, \tag{6}$$

$$\frac{\partial \Phi^{(1)}}{\partial y} = 0 \quad \text{for } x \geq 0, \ -h \leq z \leq 0, \text{ and } y = 0, b, \tag{7}$$

$$\frac{\partial \Phi^{(1)}}{\partial z} - \frac{\partial \eta^{(1)}}{\partial t} = 0 \quad \text{for } x \geq 0, \ z = 0, \text{ and } 0 \leq y \leq b, \tag{8}$$

$$\frac{\partial \Phi^{(1)}}{\partial t} + g\eta^{(1)} = B_1(t) \quad \text{for } x \geq 0, \ z = 0, \text{ and } 0 \leq y \leq b, \tag{9}$$

$$\frac{\partial \Phi^{(1)}}{\partial x} = \frac{\partial X}{\partial t} \quad \text{for } x = 0, \ -h \leq z \leq 0, \text{ and } 0 \leq y \leq b, \tag{10}$$

where g is the acceleration due to gravity.

At the second order, $\mathcal{O}(\varepsilon^2)$, the boundary-value problem describing the fluid motion may be written as

$$\nabla^2 \Phi^{(2)} = 0 \quad \text{for } x \geq 0, \ -h \leq z \leq 0, \text{ and } 0 \leq y \leq b, \tag{11}$$

$$\frac{\partial \Phi^{(2)}}{\partial z} = 0 \quad \text{for } x \geq 0, \ z = -h, \text{ and } 0 \leq y \leq b, \tag{12}$$

$$\frac{\partial \Phi^{(2)}}{\partial y} = 0 \quad \text{for } x \geq 0, \ -h \leq z \leq 0, \text{ and } y = 0, b, \tag{13}$$

$$\frac{\partial \Phi^{(2)}}{\partial z} - \frac{\partial \eta^{(2)}}{\partial t} - \frac{\partial \eta^{(1)}}{\partial x}\frac{\partial \Phi^{(1)}}{\partial x} - \frac{\partial \eta^{(1)}}{\partial y}\frac{\partial \Phi^{(1)}}{\partial y} + \eta^{(1)}\frac{\partial^2 \Phi^{(1)}}{\partial z^2} = 0$$

$$\text{for } x \geq 0,\ z = 0, \text{ and } 0 \leq y \leq b, \tag{14}$$

$$\frac{\partial \Phi^{(2)}}{\partial t} + g\eta^{(2)} + \eta^{(1)}\frac{\partial^2 \Phi^{(1)}}{\partial z \partial t} + \frac{1}{2}|\nabla \Phi^{(1)}|^2 = B_2(t) \quad \text{for } x \geq 0,\ z = 0, \text{ and } 0 \leq y \leq b, \tag{15}$$

$$\frac{\partial \Phi^{(2)}}{\partial x} - \frac{\partial \Phi^{(1)}}{\partial y}\frac{\partial X}{\partial y} - \frac{\partial \Phi^{(1)}}{\partial z}\frac{\partial X}{\partial z} + X\frac{\partial^2 \Phi^{(1)}}{\partial x^2} = 0 \quad \text{for } x = 0,\ -h \leq z \leq 0, \text{ and } 0 \leq y \leq b. \tag{16}$$

Finally, at large distances from the wave generators the potentials $\Phi^{(1)}$ and $\Phi^{(2)}$ must satisfy suitable radiation conditions which ensure the correct asymptotic behavior of the generated wave field.

3. FIRST-ORDER SOLUTION

A suitable solution to the first-order boundary problem may be written as

$$\Phi^{(1)} = \sum_{n=0}^{\infty} [\varphi_n \cos \alpha_n y\, e^{-i\omega t} + CC], \tag{17}$$

where

$$\varphi_n = \sum_{m=0}^{\infty} A_{mn} e^{-\beta_{mn} x} \frac{\cos k_m(z+h)}{\cos k_m h}, \tag{18}$$

and the wave numbers are defined by $\alpha_n = n\pi/b$, for $n = 0, 1, 2, \ldots$; the k_m are defined by $k_m = \{i\gamma_0, \gamma_1, \ldots, \gamma_m, \ldots\}$, where the γ_m for $m \geq 1$ are the positive real roots of $\omega^2 + g\gamma_m \tan \gamma_m h = 0$; and the β_{mn} are given by

$$\beta_{mn} = \begin{cases} -i\sqrt{|k_m^2 + \alpha_n^2|} & \text{if} \quad k_m^2 + \alpha_n^2 < 0, \\ \sqrt{k_m^2 + \alpha_n^2} & \text{if} \quad k_m^2 + \alpha_n^2 > 0. \end{cases} \tag{19}$$

It is noted from equation (19) that the only value of the index m that can result in an imaginary value of β_{mn} is $m = 0$. The coefficients A_{mn} appearing in equation (18) may be determined utilizing the wave-maker boundary condition, equation (10), and the orthogonality properties of the vertical eigenfunctions, and are given by

$$A_{mn} = \frac{4\varepsilon_n \omega k_m \cos k_m h}{b\beta_{mn}[2k_m h + \sin 2k_m h]}\, i \int_0^b e^{i\lambda y} \cos \alpha_n y\, dy \int_{-h}^{0} f(z) \cos k_m(z+h)\, dz, \tag{20}$$

in which $\varepsilon_0 = 1$, and $\varepsilon_n = 2$, for $n \geq 1$.

From equation (9), the corresponding water surface elevation is then given by

$$\eta^{(1)}(x, y, t) = \sum_{n=0}^{\infty} \sum_{m=0}^{\infty} \frac{\omega i}{g} A_{mn} e^{-\beta_{mn} x} \cos \alpha_n y\, e^{-i\omega t} + CC \tag{21}$$

and, by imposing a zero mean on $\eta^{(1)}(x, y, t)$ in the far field, it is found that $B_1(t) \equiv 0$. Far from the wave maker, the evanescent wave modes may be neglected and the wave profile

becomes

$$\eta^{(1)}(x, y, t) \sim \sum_{n=0}^{n^*} \frac{\omega \mathrm{i}}{g} A_{0n} \mathrm{e}^{-\beta_{0n} x} \cos \alpha_n y \, \mathrm{e}^{-\mathrm{i}\omega t} + \mathrm{CC}, \tag{22}$$

in which n^* is the maximum value of n such that $\gamma_0^2 - \alpha_n^2 > 0$.

4. SECOND-ORDER SOLUTION

The second-order free-surface boundary conditions, equations (14) and (15), may be combined to yield the following condition on $\Phi^{(2)}$ alone:

$$\varkappa(\Phi^{(2)}) = \frac{\partial^2 \Phi^{(2)}}{\partial t^2} + g \frac{\partial \Phi^{(2)}}{\partial z} = \frac{1}{g} \frac{\partial \Phi^{(1)}}{\partial t} \frac{\partial}{\partial z} \left(\frac{\partial^2 \Phi^{(2)}}{\partial t^2} + g \frac{\partial \Phi^{(2)}}{\partial z} \right) - \frac{\partial}{\partial t} (|\nabla \Phi^{(1)}|^2) + \frac{\partial B_2}{\partial t}. \tag{23}$$

It will subsequently be determined that the term $\partial B_2/\partial t$ in equation (23) is identically zero.

The second-order velocity potential will now be decomposed into complementary homogeneous and inhomogeneous solutions on the wave-maker surface and fluid-free-surface according to

$$\Phi^{(2)}(x, y, z, t) = \Phi_w^{(2)}(x, y, z, t) + \Phi_f^{(2)}(x, y, z, t), \tag{24}$$

in which $\Phi_w^{(2)}(x, y, z, t)$ is a forced wave-maker potential satisfying a homogeneous free-surface condition, and $\Phi_f^{(2)}(x, y, z, t)$ is a potential independent of the wave-maker motion which satisfies an inhomogeneous free-surface condition, namely

$$\varkappa(\Phi_w^{(2)}) = 0, \tag{25}$$

$$\varkappa(\Phi_f^{(2)}) = \varkappa(\Phi^{(2)}). \tag{26}$$

The potentials $\Phi_w^{(2)}$ and $\Phi_f^{(2)}$ can be written as

$$\Phi_w^{(2)}(x, y, z, t) = \varphi_w(x, y, z, t) \mathrm{e}^{-2\mathrm{i}\omega t} + \psi_w(x, y, z) + \mathrm{CC}, \tag{27}$$

$$\Phi_f^{(2)}(x, y, z, t) = \varphi_f(x, y, z, t) \mathrm{e}^{-2\mathrm{i}\omega t} + \psi_f(x, y, z) + \mathrm{CC}, \tag{28}$$

in which it is noted that ψ_w and ψ_f are time-independent potentials.

From equation (23) the following expression is obtained:

$$\begin{aligned} g \frac{\partial \varphi_f}{\partial z} - 4\omega^2 \varphi_f \\ = \frac{\mathrm{i}}{2} \sum_{m=0}^{\infty} \sum_{n=0}^{\infty} \sum_{j=0}^{\infty} \sum_{k=0}^{\infty} \left[\frac{3\omega^5}{g^2} + 2\omega \beta_{jm} \beta_{kn} + \omega k_k^2 - 2\omega \alpha_m \alpha_n \right] \\ \times A_{jm} A_{kn} \mathrm{e}^{-(\beta_{jm} + \beta_{kn})x} \cos(\alpha_m + \alpha_n) y \\ + \frac{\mathrm{i}}{2} \sum_{m=0}^{\infty} \sum_{n=0}^{\infty} \sum_{j=0}^{\infty} \sum_{k=0}^{\infty} \left[\frac{3\omega^5}{g^2} + 2\omega \beta_{jm} \beta_{kn} + \omega k_k^2 + 2\omega \alpha_m \alpha_n \right] \\ \times A_{jm} A_{kn} \mathrm{e}^{-(\beta_{jm} + \beta_{kn})x} \cos(\alpha_m - \alpha_n) y, \end{aligned} \tag{29}$$

$$\begin{aligned} g \frac{\partial \psi_f}{\partial z} = -\frac{\mathrm{i}}{2} \sum_{m=0}^{\infty} \sum_{n=0}^{\infty} \sum_{j=0}^{\infty} \sum_{k=0}^{\infty} \omega k_k^2 \bar{A}_{jm} A_{kn} \mathrm{e}^{-(\bar{\beta}_{jm} + \beta_{kn})x} \\ [\cos(\alpha_m + \alpha_n) y + \cos(\alpha_m - \alpha_n) y]. \end{aligned} \tag{30}$$

Equation (30) is valid for $(m-n)^2+(j-k)^2 \neq 0$. When $(m-n)^2+(j-k)^2=0$, the right-hand side of the equation becomes zero.

Suitable forms for the free-surface potentials φ_f and ψ_f are

$$\varphi_f = \sum_{m=0}^{\infty}\sum_{n=0}^{\infty}\sum_{j=0}^{\infty}\sum_{k=0}^{\infty}\left[Q(m,n,j,k)\,\mathrm{e}^{-(\beta_{jm}+\beta_{kn})x}\frac{\cos\sqrt{(\beta_{jm}+\beta_{kn})^2-(\alpha_m+\alpha_n)^2}\,(z+h)}{\cos\sqrt{(\beta_{jm}+\beta_{kn})^2-(\alpha_m+\alpha_n)^2}\,h}\right.$$

$$\times\cos(\alpha_m+\alpha_n)y$$

$$\left.+\,Q^*(m,n,j,k)\,\mathrm{e}^{-(\beta_{jm}+\beta_{kn})x}\frac{\cos\sqrt{(\beta_{jm}+\beta_{kn})^2-(\alpha_m-\alpha_n)^2}\,(z+h)}{\cos\sqrt{(\beta_{jm}+\beta_{kn})^2-(\alpha_m-\alpha_n)^2}\,h}\cos(\alpha_m-\alpha_n)y\right], \tag{31}$$

$$\psi_f = \sum_{m=0}^{\infty}\sum_{n=0}^{\infty}\sum_{j=0}^{\infty}\sum_{k=0}^{\infty}\left[E(m,n,j,k)\,\mathrm{e}^{-(\bar{\beta}_{jm}+\beta_{kn})x}\frac{\cos\sqrt{(\bar{\beta}_{jm}+\beta_{kn})^2-(\alpha_m+\alpha_n)^2}\,(z+h)}{\cos\sqrt{(\bar{\beta}_{jm}+\beta_{kn})^2-(\alpha_m+\alpha_n)^2}\,h}\right.$$

$$\times\cos(\alpha_m+\alpha_n)y$$

$$\left.+\,E^*(m,n,j,k)\,\mathrm{e}^{-(\bar{\beta}_{jm}+\beta_{kn})x}\frac{\cos\sqrt{(\bar{\beta}_{jm}+\beta_{kn})^2-(\alpha_m-\alpha_n)^2}\,(z+h)}{\cos\sqrt{(\bar{\beta}_{jm}+\beta_{kn})^2-(\alpha_m-\alpha_n)^2}\,h}\cos(\alpha_m-\alpha_n)y\right], \tag{32}$$

in which

$$Q(m,n,j,k)=\frac{-\mathrm{i}}{2g\sqrt{(\beta_{jm}+\beta_{kn})^2-(\alpha_m+\alpha_n)^2}}\,\frac{\left(\dfrac{3\omega^5}{g^2}-2\omega\alpha_m\alpha_n+2\omega\beta_{jm}\beta_{kn}+\omega k_k^2\right)A_{jm}A_{kn}}{\tan\sqrt{(\bar{\beta}_{jm}+\beta_{kn})^2-(\alpha_m+\alpha_n)^2}\,h+4\omega^2}, \tag{33}$$

$$Q^*(m,n,j,k)=\frac{-\mathrm{i}}{2g\sqrt{(\bar{\beta}_{jm}+\beta_{kn})^2-(\alpha_m-\alpha_n)^2}}$$

$$\times\frac{\left(\dfrac{3\omega^5}{g^2}+2\omega\alpha_m\alpha_n+2\omega\beta_{jm}\beta_{kn}+\omega k_k^2\right)A_{jm}A_{kn}}{\tan\sqrt{(\beta_{jm}+\beta_{kn})^2-(\alpha_m-\alpha_n)^2}\,h+4\omega^2}, \tag{34}$$

$$E(m,n,j,k)=\frac{\mathrm{i}}{2g\sqrt{(\bar{\beta}_{jm}+\beta_{kn})^2-(\alpha_m+\alpha_n)^2}}\,\frac{\omega k_k^2\bar{A}_{jm}A_{kn}}{\tan\sqrt{(\bar{\beta}_{jm}+\beta_{kn})^2-(\alpha_m+\alpha_n)^2}\,h+4\omega^2}, \tag{35}$$

$$E^*(m,n,j,k)=\frac{\mathrm{i}}{2g\sqrt{(\bar{\beta}_{jm}+\beta_{kn})^2-(\alpha_m-\alpha_n)^2}}\,\frac{\omega k_k^2\bar{A}_{jm}A_{kn}}{\tan\sqrt{(\bar{\beta}_{jm}+\beta_{kn})^2-(\alpha_m-\alpha_n)^2}\,h+4\omega^2}. \tag{36}$$

The wave-maker boundary condition at second order, equation (16), may be rearranged and written as

$$\Re[\Phi^{(2)}] = \frac{\partial \Phi^{(2)}}{\partial x} = \frac{\partial \Phi^{(1)}}{\partial y}\frac{\partial X}{\partial y} + \frac{\partial \Phi^{(1)}}{\partial z}\frac{\partial X}{\partial z} - X\frac{\partial^2 \Phi^{(1)}}{\partial x^2}$$

$$= F(y,z)\,\mathrm{e}^{-2\mathrm{i}\omega t} + T(y,z) + \mathrm{CC} \quad \text{for } x = 0,\ -h < z < 0, \quad \text{and } 0 < y < b, \tag{37}$$

where

$$F(y,z) = \sum_{n=0}^{\infty} \mathrm{e}^{\mathrm{i}\lambda y}\left[f_z \frac{\partial \varphi_n}{\partial z}\cos\alpha_n y - \mathrm{i}\lambda\alpha_n f\varphi_n \sin\alpha_n y - f\frac{\partial^2 \varphi_n}{\partial x^2}\cos\alpha_n y \right], \tag{38}$$

$$T(y,z) = \sum_{n=0}^{\infty} \mathrm{e}^{\mathrm{i}\lambda y}\left[f_z \frac{\partial \bar{\varphi}_n}{\partial z}\cos\alpha_n y - \mathrm{i}\lambda\alpha_n f\bar{\varphi}_n \sin\alpha_n y - f\frac{\partial^2 \bar{\varphi}_n}{\partial x^2}\cos\alpha_n y \right]. \tag{39}$$

Suitable forms for the wave-maker potentials φ_w and ψ_w are

$$\varphi_w = \sum_{n=0}^{\infty}\sum_{m=0}^{\infty} B_{mn}\,\mathrm{e}^{-\mu_{mn}x}\frac{\cos\xi_m(z+h)}{\cos\xi_m h}\cos\alpha_n y, \tag{40}$$

$$\psi_w = \sum_{n=0}^{4}\sum_{m=0}^{4} C_{mn}\,\mathrm{e}^{-\upsilon_{mn}x}\frac{\cos\zeta_m(z+h)}{\cos\zeta_m h}\cos\alpha_n y, \tag{41}$$

where the wave numbers are defined by $\zeta_m = m\pi/b$, for $m \geq 0$; the ξ_m are defined by $\xi_m = \{\mathrm{i}\sigma_0, \sigma_1, \ldots, \sigma_m, \ldots\}$, where σ_0 is the positive real root of $4\omega^2 = g\sigma_0 \tanh\sigma_0 h$; the σ_m for $m > 1$ are the positive real roots of $4\omega^2 + g\sigma_m \tan\sigma_m h = 0$; and the μ_{mn} and the υ_{mn} are given by

$$\mu_{mn} = \begin{cases} -\mathrm{i}\sqrt{|\xi_m^2 + \alpha_n^2|} & \text{if} \quad \xi_m^2 + \alpha_n^2 < 0, \\ \sqrt{\xi_m^2 + \alpha_n^2} & \text{if} \quad \xi_m^2 + \alpha_n^2 > 0, \end{cases} \tag{42}$$

$$\upsilon_{mn} = \sqrt{\zeta_m^2 + \alpha_n^2}\,. \tag{43}$$

It is noted from equation (42) that the only value of the index m that can result in an imaginary value of μ_{mn} is $m = 0$.

The potential coefficients appearing in equations (40) and (41) may be determined through the modified second-order wave-maker boundary condition, namely

$$\Re[\Phi_w^2] = \Re[\Phi^2] - \Re[\Phi_f^2], \tag{44}$$

and the orthogonality properties of the vertical eigenfunctions. The potential coefficients may be written as

$$B_{mn} = \frac{4\varepsilon_n \xi_m \cos\xi_m h}{b\mu_{mn}(\sin 2\xi_m h + 2\xi_m h)}\left\{ \int_{-h}^{0}\left[\int_0^b \left(\left.\frac{\partial \varphi_f}{\partial x}\right|_{x=0} - F(y,z)\right)\cos\alpha_n y\,\mathrm{d}y \right] \times \cos\xi_m(z+h)\,\mathrm{d}z \right\}, \tag{45}$$

$$C_{mn} = \frac{\varepsilon_m \varepsilon_n \cos\zeta_m h}{b\upsilon_{mn} h}\left\{ \int_{-h}^{0}\left[\int_0^b \left(\left.\frac{\partial \psi_f}{\partial x}\right|_{x=0} - T(y,z)\right)\cos\alpha_n y\,\mathrm{d}y \right] \times \cos\zeta_m(z+h)\,\mathrm{d}z \right\}. \tag{46}$$

The second-order free-surface elevation $\eta^{(2)}(x, y, t)$ may now be obtained by rearranging equation (15) to give

$$\eta^{(2)} = -\frac{1}{g}\frac{\partial \Phi^{(2)}}{\partial t} + \frac{1}{g^2}\frac{\partial \Phi^{(1)}}{\partial t}\frac{\partial^2 \Phi^{(1)}}{\partial z\,\partial t} - \frac{1}{2g}|\nabla \Phi^{(1)}|^2 + \frac{B_2(t)}{g} \quad \text{for } x \geq 0,\ 0 \leq y \leq b,\ z = 0. \tag{47}$$

The Bernoulli constant at second order, $B_2(t)$, is calculated by imposing a zero mean on $\eta^{(2)}(x, y, t)$ in the far field, and is found to be

$$B_2(t) = \sum_{n=0}^{n^*} \frac{|A_{0n}|^2 |k_0|^2}{\varepsilon_n \cos^2 k_0 h}. \tag{48}$$

At large distances from the wave maker, the evanescent wave modes may be neglected and the second-order water surface profile becomes

$$\begin{aligned}\eta^{(2)}(x, y, t) \sim & \sum_{m=0}^{n^*}\sum_{n=0}^{n^*} \left\{ \left[\frac{2\mathrm{i}\omega}{g} Q(m, n, 0, 0) - \left(\frac{3\omega^4}{4g^3} + \frac{\beta_{0m}\beta_{0n}}{4g} - \frac{\alpha_m \alpha_n}{4g} \right) A_{0m} A_{0n} \right] \right. \\ & \times \cos(\alpha_m + \alpha_n) y \\ & \left. + \left[\frac{2\mathrm{i}\omega}{g} Q^*(m, n, 0, 0) - \left(\frac{3\omega^4}{4g^3} + \frac{\beta_{0m}\beta_{0n}}{4g} + \frac{\alpha_m \alpha_n}{4g} \right) A_{0m} A_{0n} \right] \cos(\alpha_m - \alpha_n) y \right\} \\ & \times \mathrm{e}^{-[(\beta_{0m} + \beta_{0n})x + 2\mathrm{i}\omega t]} + \sum_{m=0}^{n^*}\sum_{n=0}^{n^*} \left\{ \left(\frac{3\omega^4}{4g^3} - \frac{\bar{\beta}_{0m}\beta_{0n}}{4g} + \frac{\alpha_m \alpha_n}{4g} \right) \cos(\alpha_m + \alpha_n) y \right. \\ & \left. + \left(\frac{3\omega^4}{4g^3} - \frac{\bar{\beta}_{0m}\beta_{0n}}{4g} - \frac{\alpha_m \alpha_n}{4g} \right) \cos(\alpha_m - \alpha_n) y \right\} \bar{A}_{0m} A_{0n} \mathrm{e}^{-(\bar{\beta}_{0m} + \beta_{0n})x} \\ & + \sum_{n=0}^{n^*} \frac{2\mathrm{i}\omega}{g} B_{0n} \cos \alpha_n y\, \mathrm{e}^{-(\mu_{0n} x + 2\mathrm{i}\omega t)} + \sum_{n=0}^{n^*} \frac{|A_{0n}|^2 |k_0|^2}{g\varepsilon_n \cos^2 k_0 h} + \mathrm{CC}, \end{aligned} \tag{49}$$

in which n^* is the maximum value of m such that $\sigma_0^2 - \alpha_n^2 > 0$.

5. NUMERICAL EXAMPLES

The correctness of the present theory and the associated computer program is first verified through comparisons with two limiting solutions appearing in the open literature. Figure 2 presents a comparison of the first-order solution for water surface elevation in the tank, obtained by the eigenfunction expansion approach, with the Greens function solution of Williams & Crull (1996). These results are for an array of full-draft flap-type wave makers, whose displacements are defined by

$$X(y, z, t) = A_0(1 + z/h)\,\mathrm{e}^{\mathrm{i}(\lambda_0 y - \omega t)} + \mathrm{CC}, \tag{50}$$

where A_0 is the amplitude of the wave-maker stroke at the still water level. The water surface elevation in the figure is nondimensionalized by A_0 and L is the wavelength, $L = 2\pi/\gamma_0$. The first-order solution was obtained by truncating the infinite series in the expressions for the potential after 20 terms; increasing the number of terms to 40 did not change the solution by more than 1%, indicating that convergence had essentially been

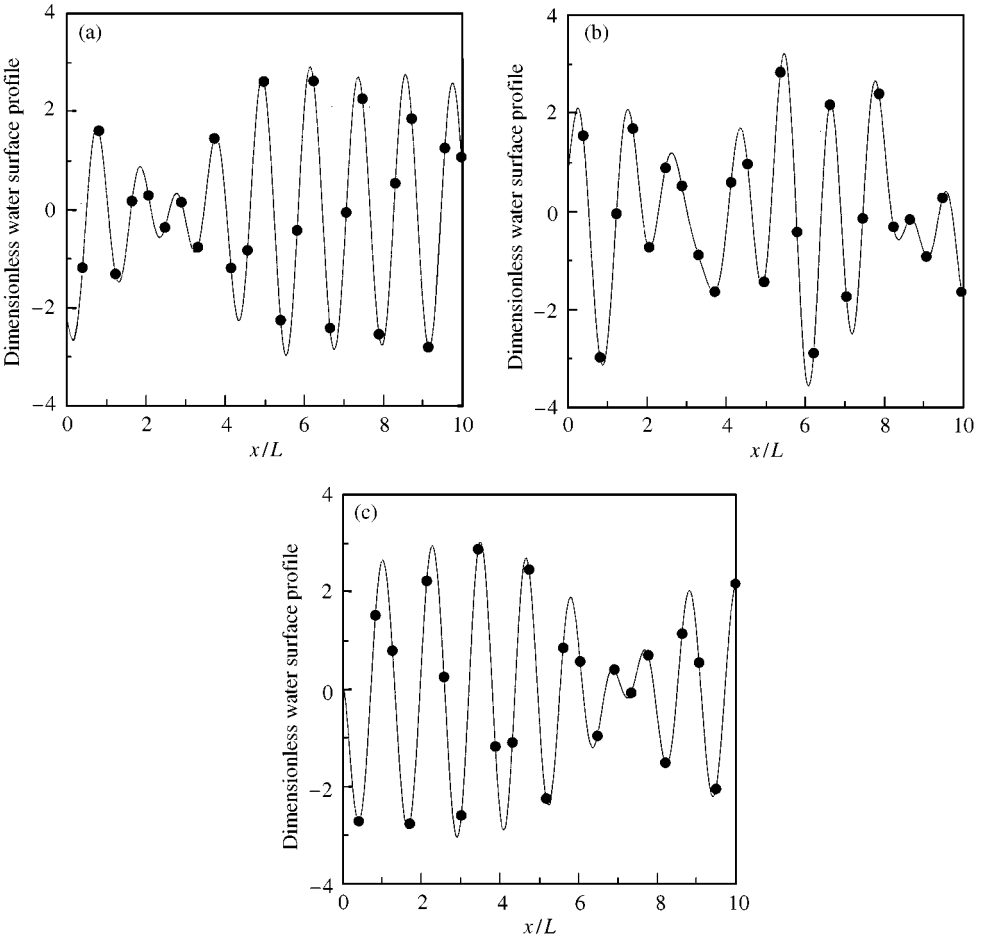

Figure 2. Comparison of dimensionless first-order water surface profiles at $t = 0$ obtained by present approach [lines] with results of Williams & Crull (1996) (symbols) for $h/b = 1$, $b/L = 1{\cdot}6$ and $\theta = 30°$: (a) $y = b/4$; (b) $y = b/2$; (c) $y = 3b/4$.

achieved. Comparisons are presented at $y = b/4$, $b/2$ and $3b/4$, and it can be seen that the agreement is excellent at each location. Figure 3 presents a comparison of the ratios of the amplitudes of the second-order, far-field, free (wave maker) to the forced (free-surface) wave elevations with the two-dimensional solution of Sulisz & Hudspeth(1993a). The two curves correspond to the inclusion, or neglect, of the second-order evanescent interaction potential arising from the evanescent wave terms at first order. The first- and second-order solutions were obtained by truncating the infinite series in the expressions for the potentials after 20 and 40 terms, respectively. Again, increasing the number of terms beyond 40 did not change the second-order solution by more than 1–2%. Excellent agreement is observed over the entire range of interest. The dimensionless wavenumber on the horizontal axis is h/L, where L is the first-order wavelength defined above.

Several numerical examples are now presented that illustrate the influence of wave angle and basin width on the generated wave field. In all of the following cases, the waves are produced by an array of full-draft flap-type wave makers of stroke $A_0 = 0{\cdot}2$ m oscillating at

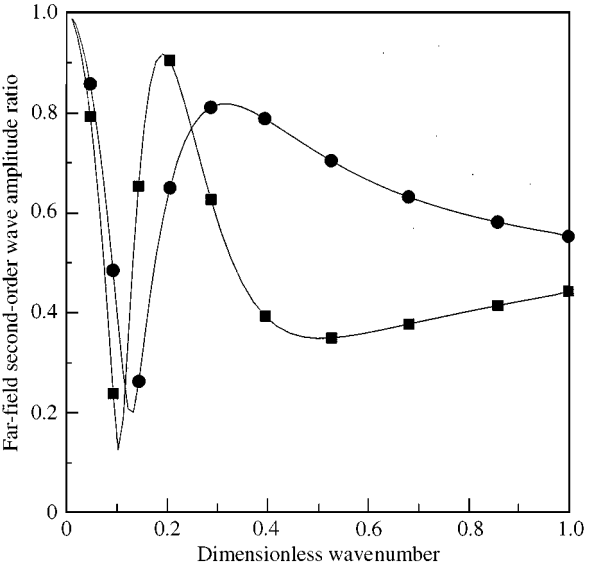

Figure 3. Comparison of ratios of amplitude of second-order wave maker induced to free-surface induced far-field wave amplitudes obtained by present approach (lines) with results of Sulisz & Hudspeth (1993a) (symbols) for full-draft flap-type wave maker. Notations: ■ with evanescent interaction potential; ● without evanescent interaction potential.

a period $T = 2{\cdot}2$ s, and the water depth $h = 5$ m. Based on the above numerical comparisons, all numerical results have been obtained by truncating the infinite series in the expressions for the first- and second-order potentials after 20 and 40 terms, respectively. In the figures, the wave generators are located at $x = 0$, and the x- and y-coordinates have been nondimensionalized by the wavelength L. The water-surface elevation is dimensional.

Figure 4 presents the instantaneous first-order, second-order and total (first plus second-order) water-surface elevations at $t = 0$, for a basin width $b = 20$ m, and wave heading $\theta = 30^\circ$. The form of the first- and second-order wave fields can clearly be seen in the figure. In particular, the reflection of the waves from the sidewall of the tank is shown. In this example, the maximum first-order wave elevation is 0·87 m, while the maximum second-order wave elevation is 0·22 m. These maxima occur along the tank wall $y = b$ where the primary wave reflection is occurring. The maximum total (first- plus second-order) surface elevation at this location is 1·08 m. Figures 5 and 6 present the instantaneous first-order, second-order and total (first- plus second-order) water surface elevations at $t = 0$ for basin widths $b = 35$ and 50 m, respectively. By comparing Figures 4, 5, and 6, it can be seen that as the tank width is increased, the wave reflections from the sidewalls are more clearly apparent. For the 35 m tank (Figure 5), the maximum first-order wave elevation is 0·79 m, while the maximum second-order wave elevation is 0·26 m. Again, these maxima occur along the tank wall $y = b$ and the maximum total (first- plus second-order) surface elevation at this instant is 0·98 m. The corresponding values of the first-order, second-order and total surface elevation maxima in Figure 6 are 0·82, 0·19, and 0·99 m, respectively.

Figure 7 presents the instantaneous first-order, second-order and total (first- plus second-order) water surface elevations at $t = 0$ for a wave heading $\theta = 45^\circ$ and a basin width $b = 50$ m. In Figure 7, the maximum first-order wave elevation is 0·97 m, and the maximum second-order wave elevation is 0·32 m. The maximum total (first- plus second-order) surface elevation at this instant is 1·28 m. Again, reflection of both the first- and second-order waves

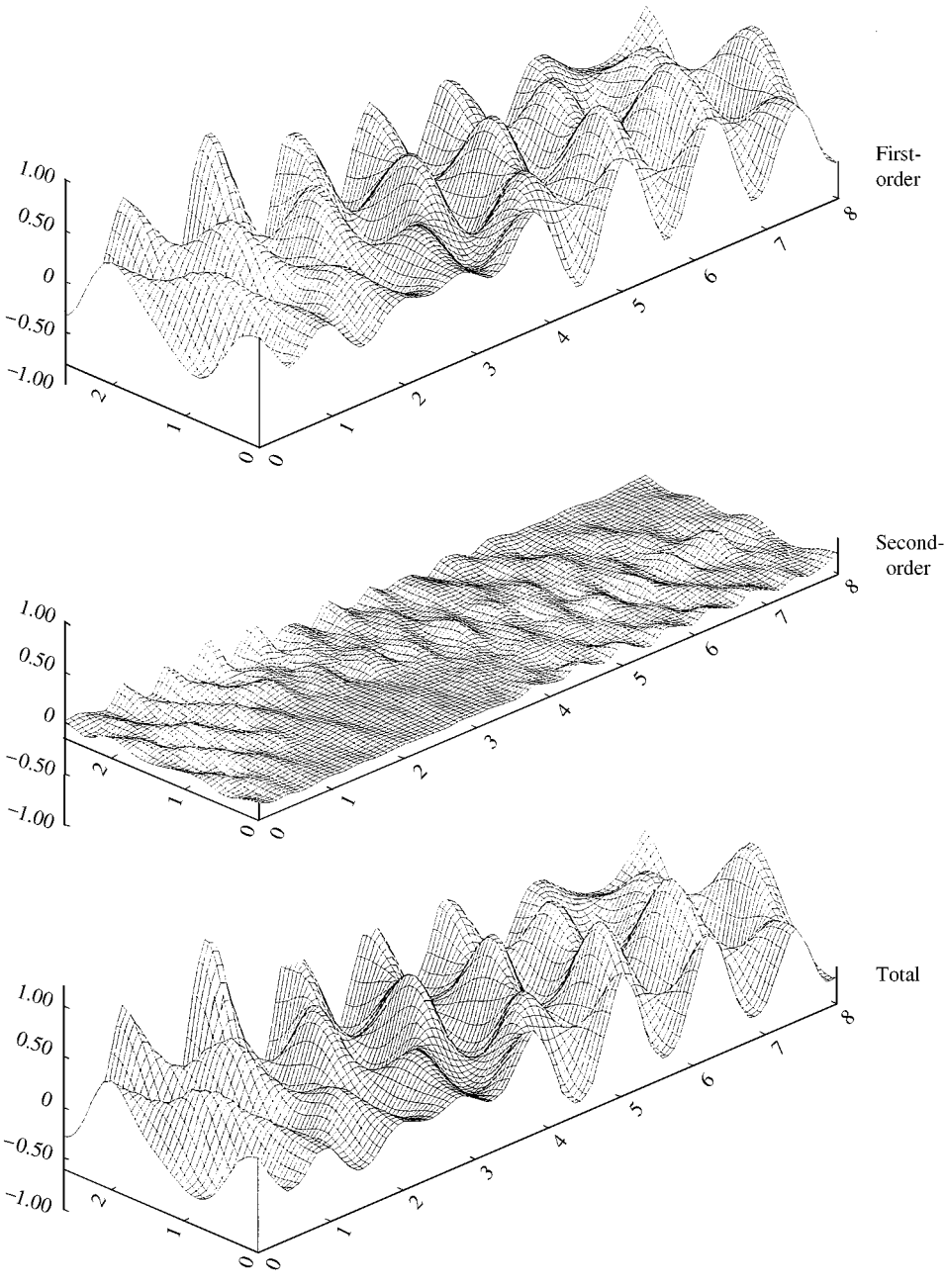

Figure 4. Instantaneous first-order (top), second-order (middle) and total (bottom) water surface elevations at $t = 0$ for $A_0 = 0{\cdot}2$ m, $T = 2{\cdot}2$ s, $h = 5$ m, $b = 20$ m and $\theta = 30°$.

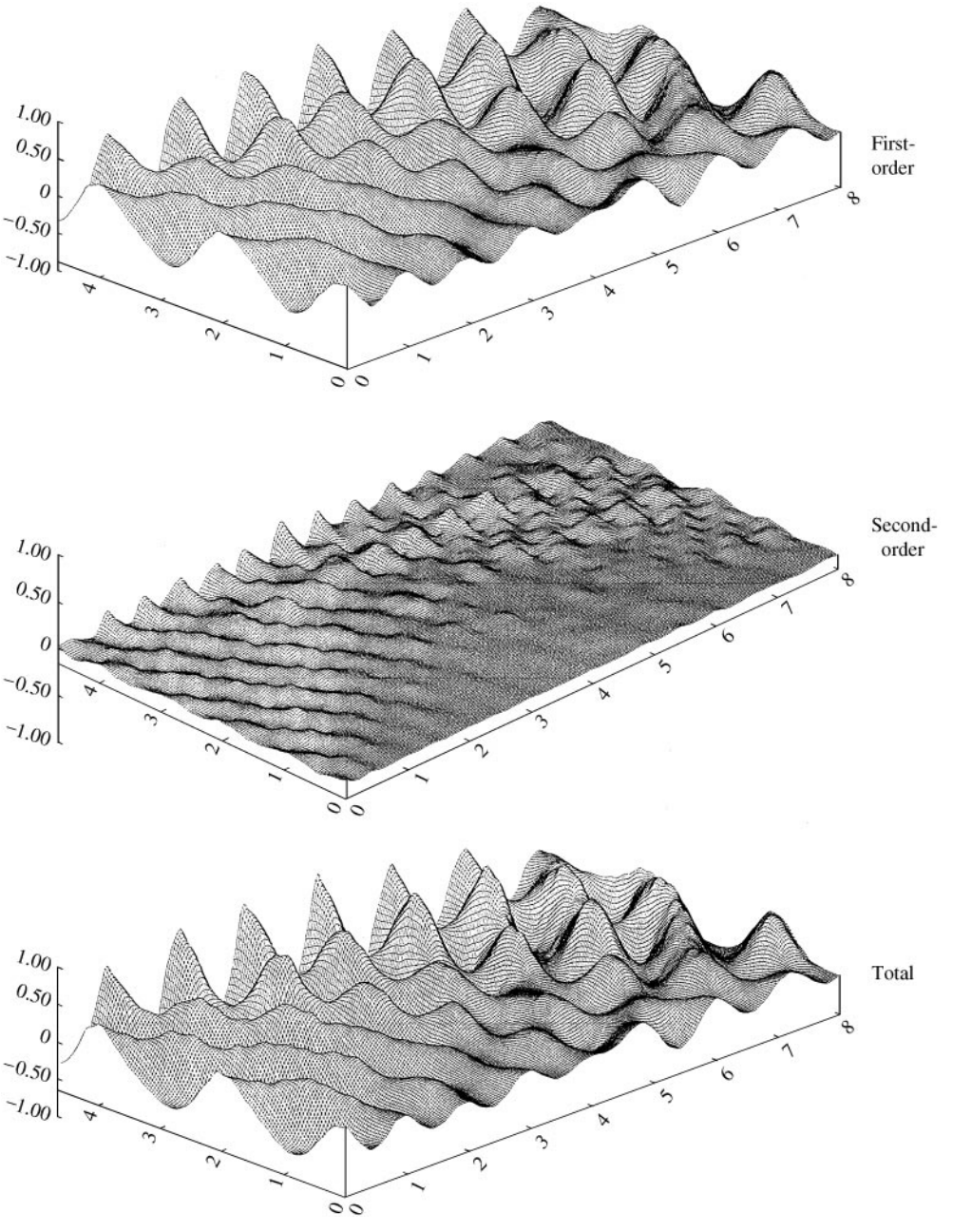

Figure 5. Instantaneous first-order (top), second-order (middle) and total (bottom) water surface elevations at $t = 0$ for $A_0 = 0{\cdot}2$ m, $T = 2{\cdot}2$ s, $h = 5$ m, $b = 35$ m and $\theta = 30^\circ$.

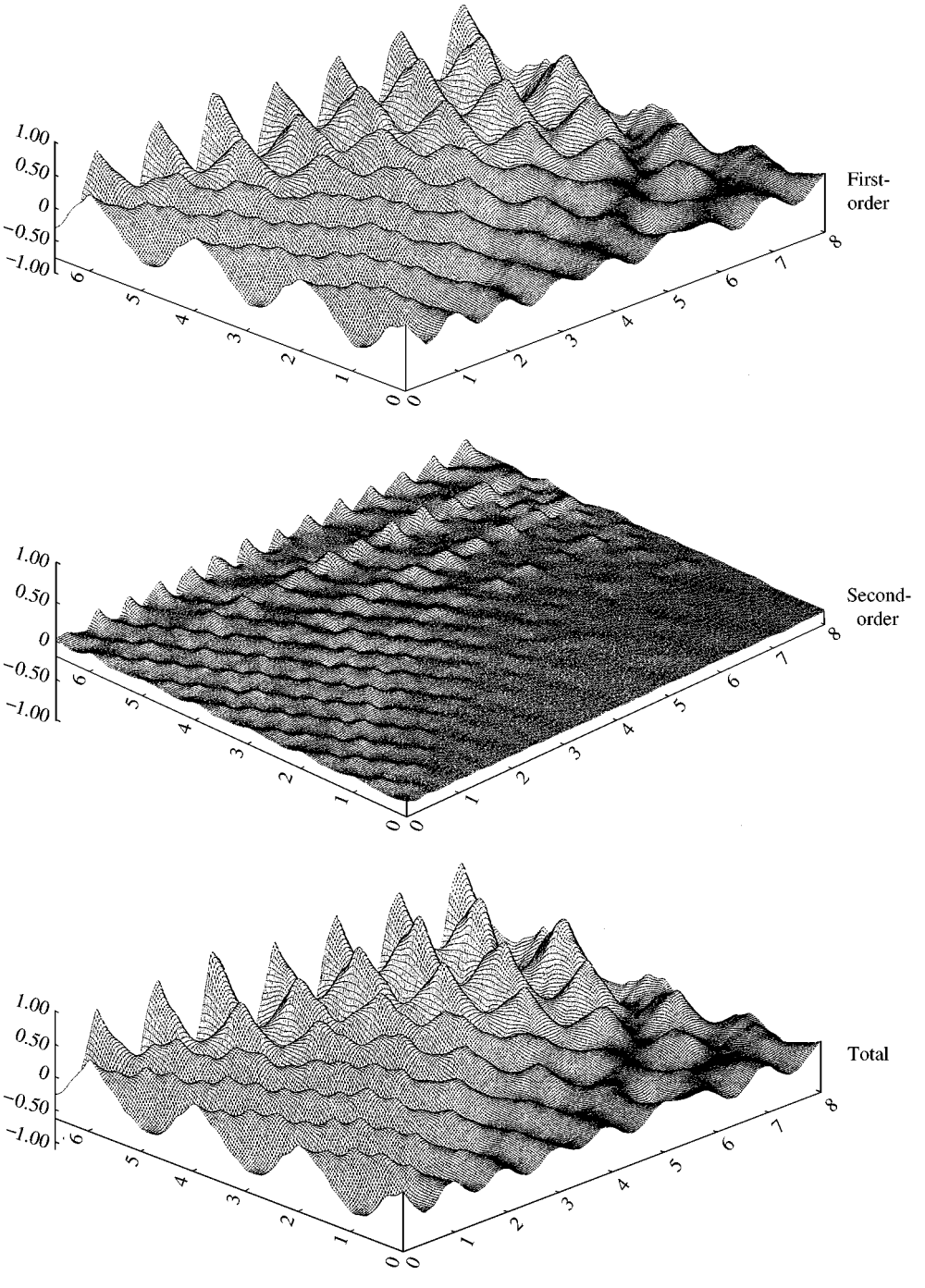

Figure 6. Instantaneous first-order (top), second-order (middle) and total (bottom) water surface elevations at $t = 0$ for $A_0 = 0{\cdot}2$ m, $T = 2{\cdot}2$ s, $h = 5$ m, $b = 50$ m and $\theta = 30^\circ$.

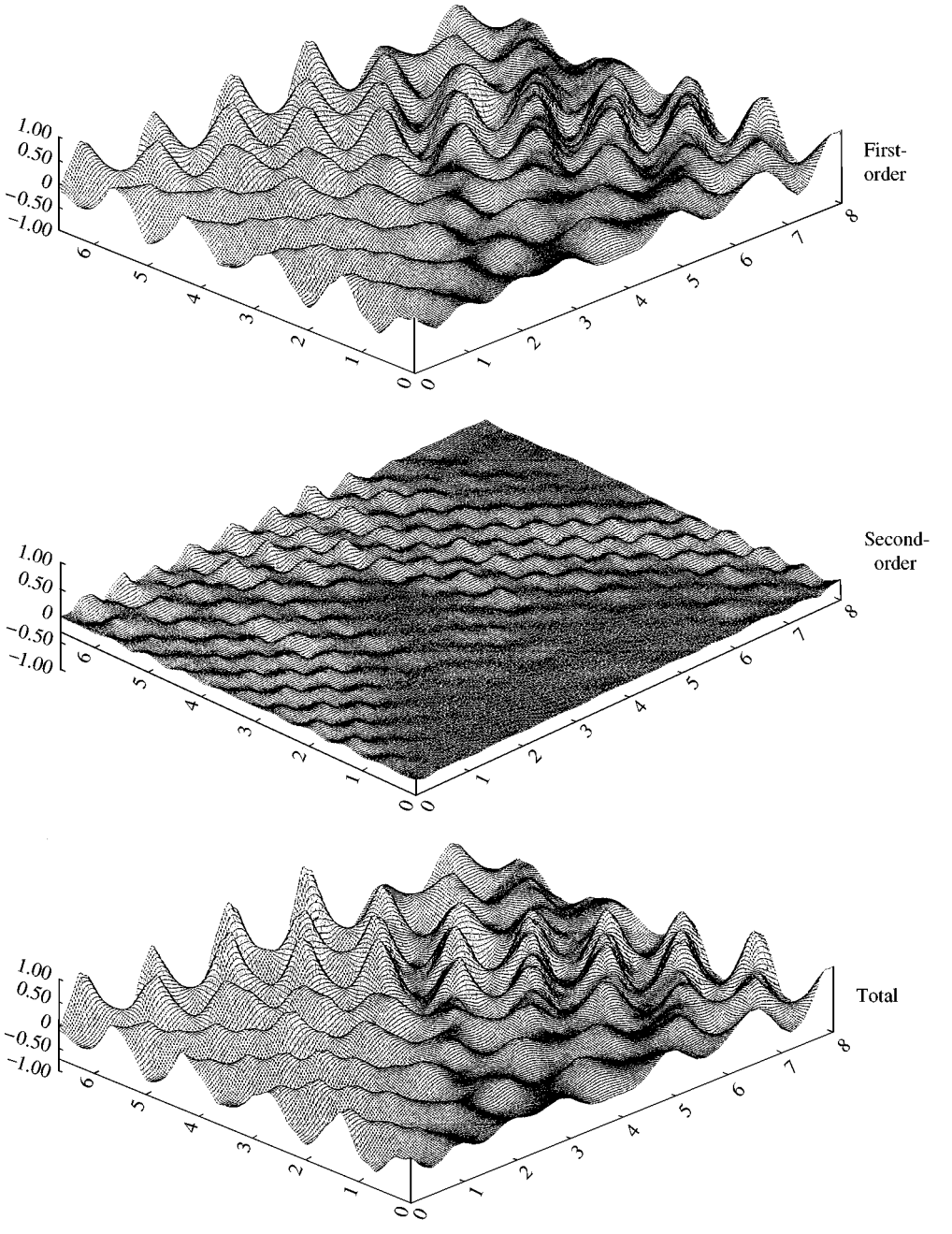

Figure 7. Instantaneous first-order (top), second-order (middle) and total (bottom) water surface elevations at $t = 0$ for $A_0 = 0{\cdot}2$ m, $T = 2{\cdot}2$ s, $h = 5$ m, $b = 50$ m and $\theta = 45^\circ$.

from the tank walls can clearly be seen. The results in this figure may be compared directly with those in Figure 5, where the wave heading $\theta = 30^\circ$, in order to illustrate the influence of wave heading on the numerical results. As intuitively expected, the $\theta = 45^\circ$ case, which results in a higher angle of wave incidence on the sidewall, yields larger maxima on the sidewall due to the reflection process.

The relative contributions of the second-order components to the total wave field are further illustrated in Figures 8 and 9, which present the instantaneous first- order, second-order and total (first- plus second-order) water surface elevations at $t = 0$ at longitudinal

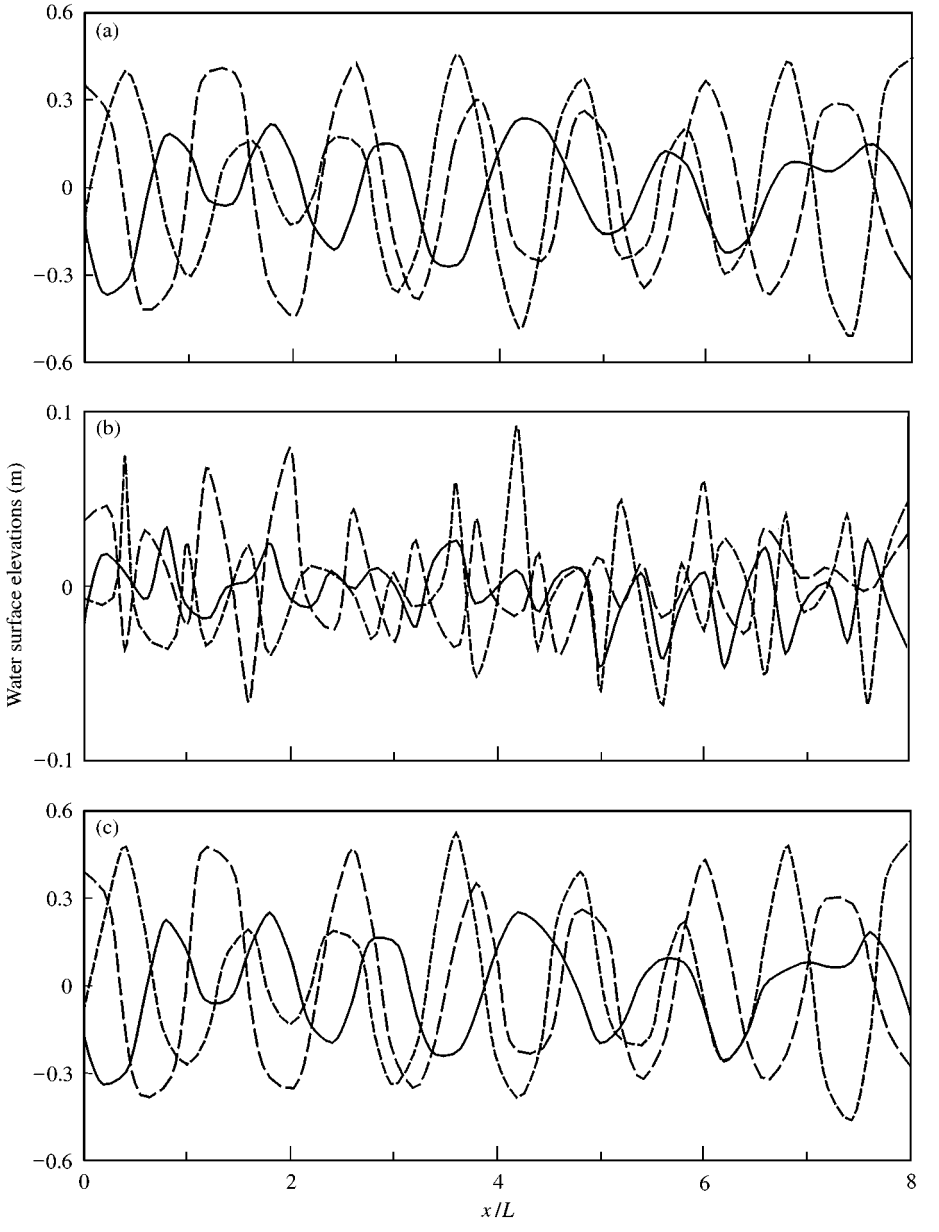

Figure 8. (a) First-order (b), second-order, and (c) total, water surface elevations at $t = 0$ for $A_0 = 0{\cdot}2$ m, $T = 2{\cdot}2$ s, $h = 5$ m, $b = 20$ m and $\theta = 30^\circ$. Notation: ——, $y = b/4$; - - - -, $y = b/2$; ----,$y = 3b/4$.

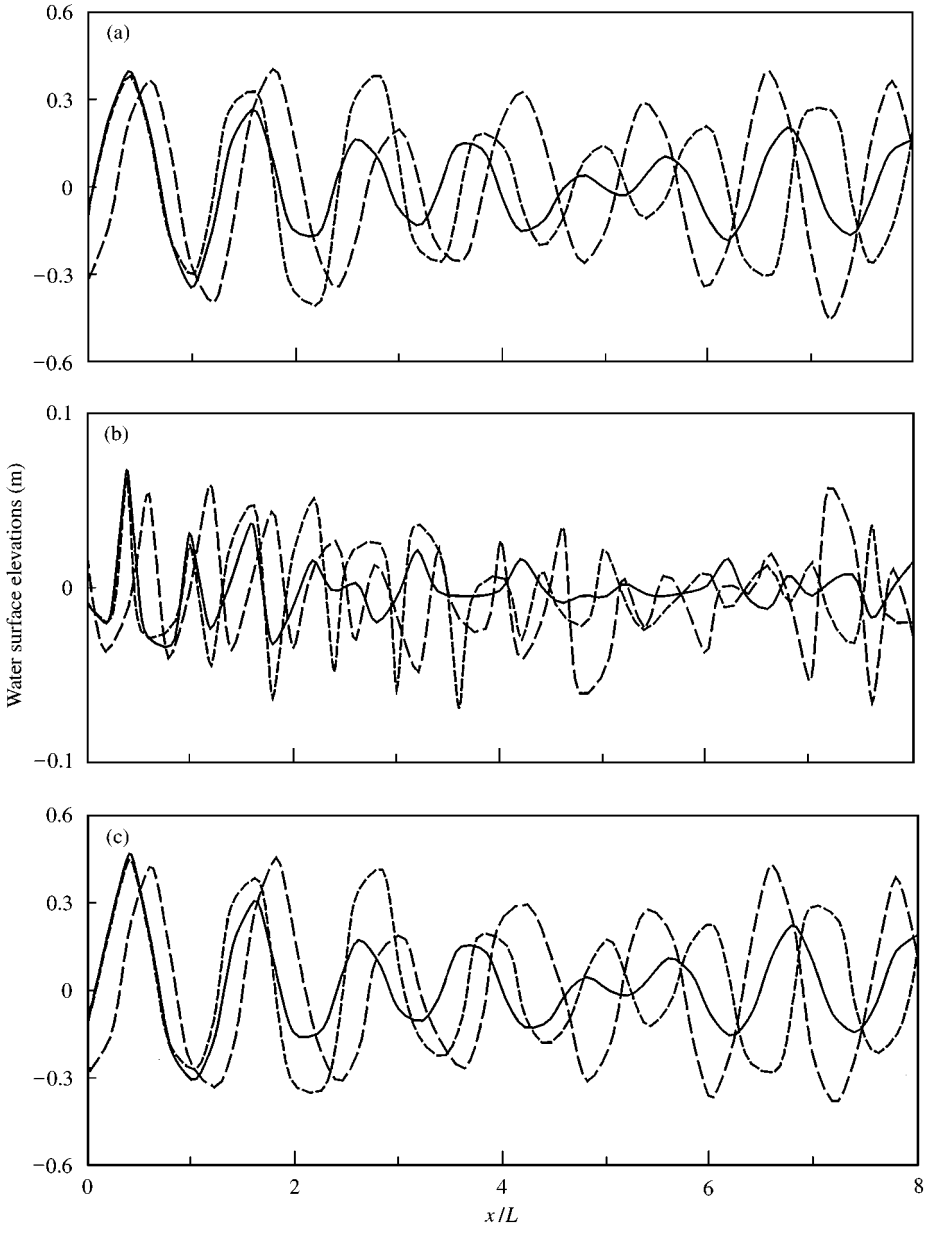

Figure 9. (a)First-order, (b) second-order, and (c) total water surface elevations at $t = 0$ for $A_0 = 0{\cdot}2$ m, $T = 2{\cdot}2$ s, $h = 5$ m, $b = 50$ m and $\theta = 30^\circ$. Notation: ———, $y = b/4$, - - - -, $y = b/2$, ------, $y = 3b/4$.

sections along the tank, defined by $y = b/4$, $b/2$, and $3b/4$. The results in Figure 8 correspond to a basin width $b = 20$ m while those in Figure 9 are for the widest basin studied, $b = 50$ m. In both cases the wave heading is $\theta = 30^\circ$. It can be seen that because of the wave direction, for a given x-location in the wave tank the surface elevations are, in general, larger at $y = 3b/4$, i.e., closer to the sidewalls. Furthermore, it is noted that the second-order effects in the narrower tank (Figure 8) exhibit peak values larger than those in the wider tank (Figure 9), and these differences are evident in the estimates of the total elevations.

6. CONCLUSIONS

A complete second-order solution has been presented for the wave field generated by the snake-like motion of an array of wave generators located at one end of a semi-infinite rectangular basin. The solutions to the boundary-value problems at first and second order are obtained by the method of eigenfunction expansions. The solution has been verified against previously existing solutions in two limiting cases: a first-order solution for wave generation in a three-dimensional basin and a second-order solution for wave generation in a narrow flume. Example results have been presented which illustrate the influence of the wave heading and basin width on the generated wave field. It has been found that due to sidewall reflection the basic characteristics of the wave field in the basin may differ significantly from the desired wave conditions, and that different transverse locations in the tank located at the same downstream distance from the wave generators may experience different wave conditions.

The present theory has several applications. For example, it could be used to identify that region of a given wave basin applicable for testing by comparing actual wave conditions with target plane-wave conditions, or it could be used to develop an algorithm that utilizes sidewall reflections to enhance the testing area of the basin under steep wave conditions (where second-order effects are important). Finally, the complete second-order solution presented herein also forms a starting point for the development of a second-order wave-maker signal to eliminate spurious second-order wave components in three-dimensional directional wave basins.

REFERENCES

DALRYMPLE, R. A. 1989 Directional wave maker theory with sidewall reflection. *Journal of Hydraulic Research*, **27,** 23–34.

DAUGAARD, E. 1972 Generation of regular waves in the laboratory. Doctoral Dissertation, Institute of Hydrodynamics Engineering, Technical University of Denmark.

DEAN, R. G. & DALRYMPLE, R. A. 1984 *Water Wave Mechanics for Scientists and Engineers.* Englewood Cliffs: Prentice-Hall.

FLICK, R. E. & GUZA, R. T. 1980 Paddle generated waves in laboratory channels. *ASCE Journal of Waterway, Port, Coastal and Ocean Engineering*, **106,** 71–97.

FUNKE, E. R. & MILES, M. D. 1987 Multi-directional wave generation with corner reflectors. Technical Report No. TR-HY-021, National Research Council Hydraulics Laboratory, Ottawa, Canada.

HUDSPETH, R. T. & SULISZ, W. 1991 Stokes drift in two-dimensional wave flumes. *Journal of Fluid Mechanics* **230,** 209–229.

ISAACSON, M. 1995 Wave field in a laboratory wave basin with partially reflecting boundaries. *International Journal of Offshore and Polar Engineering* **5,** 1–9.

MADSEN, O. S. 1971 On the generation of long waves. *Journal of Geophysical Research* **76**, 8672–8683.

MOUBAYED, W. I. & WILLIAMS, A. N. 1994 Second-order bichromatic waves produced by a generic planar wave maker in a two-dimensional wave flume. *Journal of Fluids and Structures*, **8,** 73–92.

OTTESEN-HANSEN, N. E., SAND, S. E., LUNDGREN, H., SORENSEN, T. and GREVESEN, H. 1980 Correct reproduction of group-induced long waves. *Coastal Engineering* **7,** 784–800.

SAND, S. E. 1982 Wave grouping described by bounded long waves. *Ocean Engineering*, **9,** 567–580.

SAND, S. E. & MANSARD, E. P. D. 1986 Reproduction of higher harmonics in irregular waves. *Ocean Engineering* **13,** 57–83.

SCHAFFER, H. A. 1996 Second-order wave maker theory for irregular waves. *Ocean Engineering* **23,** 47–88.

SULISZ, W. & HUDSPETH, R. T. 1993a Complete second-order solution for water waves generated in wave flumes. *Journal of Fluids and Structures* **7,** 253–268.

SULISZ, W. & HUDSPETH, R. T. 1993b Second-order wave loads on planar wave makers. *ASCE Journal of Waterway, Port, Coastal and Ocean Engineering*, **119,** 521–536.

WILLIAMS, A. N. & CRULL, W. W. 1996 Analysis of directional waves in a laboratory basin by a non-singular integral equation approach. *Proceedings ISOPE'96 Conference*, Los Angeles, California.

ZHANG, S. & WILLIAMS, A. N. 1996 Time-domain simulation of the generation and propagation of second-order Stokes waves in a two-dimensional wave flume. Part I: monochromatic wave maker motions. *Journal of Fluids and Structures* **10,** 319–335.

ZHANG, S. & WILLIAMS, A. N. 1999 Simulation of bichromatic second-order Stokes waves in a numerical wave flume. *International Journal of Offshore and Polar Engineering*, **9**, 175–181.